remote sensing

MDPI

Article

UAV-Based Characterization of Tree-Attributes and Multispectral Indices in an Uneven-Aged Mixed Conifer-Broadleaf Forest

Eduardo D. Vivar-Vivar [1], Marín Pompa-García [2,*], José A. Martínez-Rivas [2] and Luis A. Mora-Tembre [3]

[1] Maestría en Geomática Aplicada a Recursos Forestales y Ambientales, FCFyA, Universidad Juárez del Estado de Durango, Río Papaloapan y Blvd, Durango Valle del Sur s/n, Durango 34120, Mexico; unam.vivar@gmail.com
[2] Laboratorio de Dendroecología, FCFyA, Universidad Juárez del Estado de Durango, Río Papaloapan y Blvd, Durango Valle del Sur s/n, Durango 34120, Mexico; mtz.alexis05@gmail.com
[3] Secretaría de Ecología y Medio Ambiente del Estado de Quintana Roo, Efraín Aguilar Núm. 418, Col. Campestre de la Ciudad de Chetumal, Chetumal 77030, Mexico; krotalo25@gmail.com
* Correspondence: mpgarcia@ujed.mx; Tel.: +52-61-81-301096

Abstract: Unmanned aerial vehicles (UAVs) have contributed considerably to forest monitoring. However, gaps in the knowledge still remain, particularly for natural forests. Species diversity, stand heterogeneity, and the irregular spatial arrangement of trees provide unique opportunities to improve our perspective of forest stands and the ecological processes that occur therein. In this study, we calculated individual tree metrics, including several multispectral indices, in order to discern the spectral reflectance of a natural stand as a pioneer area in Mexican forests. Using data obtained by UAV DJI 4, and in the free software environments OpenDroneMap and QGIS, we calculated tree height, crown area, number of trees and multispectral indices. Digital photogrammetric procedures, such as the ForestTools, Structure from Motion and Multi-View Stereo algorithms, yielded results that improved stand mapping and the estimation of stand attributes. Automated tree detection and quantification were limited by the presence of overlapping crowns but compensated by the novel stand density mapping and estimates of crown attributes. Height estimation was in line with expectations (R^2 = 0.91, RMSE = 0.36) and is therefore a useful parameter with which to complement forest inventories. The diverse spectral indices applied yielded differential results regarding the potential vegetation activity present and were found to be complementary to each other. However, seasonal monitoring and careful estimation of photosynthetic activity are recommended in order to determine the seasonality of plant response. This research contributes to the monitoring of natural forest stands and, coupled with accurate in situ measurements, could refine forest productivity parameters as a strategy for the validity of results. The metrics are reliable and rapid and could serve as model inputs in modern inventories. Nevertheless, increased efforts in the configuration of new technologies and algorithms are required, including full consideration of the costs implied by their adoption.

Keywords: index vegetation; UAV; natural forest; estimation attributes; forest productivity; crown delineation; automated tree detection

Citation: Vivar-Vivar, E.D.; Pompa-García, M.; Martínez-Rivas, J.A.; Mora-Tembre, L.A. UAV-Based Characterization of Tree-Attributes and Multispectral Indices in an Uneven-Aged Mixed Conifer-Broadleaf Forest. *Remote Sens.* **2022**, *14*, 2775. https://doi.org/10.3390/rs14122775

Academic Editor: Nikolay Strigul

Received: 21 April 2022
Accepted: 7 June 2022
Published: 9 June 2022

1. Introduction

Accurate forest ecosystem monitoring has become a constant among the requirements of large-scale environmental projects [1]. For example, the scientific community seeks improved inputs for models of monitoring greenhouse gases [2] and estimation of carbon and biomass storage [3], among others, including reducing emissions from deforestation and forest degradation (REDD) [4].

Remote sensing technology has become more flexible in recent years and offers a promising perspective [5]. At present, it is not only possible to obtain a greater spatial

resolution of attributes that are visible to the naked eye, but also to detect multispectral attributes beyond the visible spectrum [6–8]. For example, experimentation with radiation emitted by the multispectral indices is crucial to further our understanding of ecological mechanisms that remain unclear, particularly in heterogeneous forests [9]. To this end, the application of drone technology has been rapidly extended at small and medium scales [10], including in the acquisition of highly accurate estimates at the individual tree level that serves to improve forest management [11,12]. As a result, direct and destructive estimates, which are normally so time-consuming, have been substituted by indirect estimates, such as those obtained by using unmanned aerial vehicles (UAV), with the opportunities offered by near-real-time monitoring with multiple sensors [13].

The Mexican Sierra Madre Occidental is known to occupy a special place in forest diversity [14], where different conifer and broadleaf species coexist within a small site. These areas constitute natural laboratories for gathering scientific knowledge regarding dendroecological attributes, including the use of multispectral indices since these can reflect different ecological inter-relationships [15]. For example, the estimation of structural attributes to individual tree levels, such as height and crown area, is of great utility for forest inventories and the determination of biomass and carbon values [3]. For their part, the multispectral indices are indicators of crown vigor, phenology, structural characteristics, defoliation risk and photosynthesis rates, among other variables of forest productivity [16,17]. Monitoring of these variables in complex, unevenly aged and mixed forests can therefore offer new elements for decision-making on the part of forest managers [18], considering that these systems are the greatest reservoirs of carbon and are widely representative of the Mexican forests.

Although different studies have estimated the structural attributes of heterogeneous forests [19], few have integrated the evaluation of spectral attributes [20]. Moreover, estimation of aerial structures in natural forests remains a challenge [11].

For this reason, a complete census of the trees in a pilot site was conducted in order to evaluate the capacity of a UAV to (1) calculate the metrics of tree height, crown area and the number of trees, and (2) examine the applicability of multispectral indices for monitoring in a mixed and heterogeneous stand of conifer and broadleaf species in northern Mexico. We hypothesized that the UAV will provide reliable information pertaining to the attributes of individual trees, thus serving to improve our future perspective of the vegetation properties.

2. Materials and Methods

The study site is found in the area known as "El Cordoncito" in Mesa de Pawiranachi, in the municipality of Guachochi, in the Sierra Madre Occidental mountain range of northern Mexico (27°80′5700N, 107°60′4100W; 2400 masl) (Figure 1).

Located in the region of the Holarctic and Neotropical transition, the zone presents a great complexity of ecosystems predominated by pine and oak forests, as a consequence of the variables of physiography and climatic units. This region supplies more than 25% of the timber production in Mexico, and is one of the most important timber reserves in the country, provides a wide variety of environmental services and has a predominantly indigenous population [21]. The vegetation includes forests of pine-oak species, such as *Pinus engelmannii* Carr., *P. arizonica Engelm*., *P. leiophylla* Schiede ex Schltdl. &; Cham., *Quercus arizonica* Sarg., *Q. crassifolia* Humb. &; Bonpl. and *Q. durifolia* Seemen ex Loes., as well other broadleaf species including *Arbutus arizonica* (A. Gray) Sarg.; *A. bicolor* S. González, M. González &; P.D. Sørensen; *Juniperus deppeana* Steud. There are also patches of tropical montane cloud forest and communities such as chaparral (primary and secondary) and forest clearing vegetation [14]. The dominant soils are Regosols and Leptosols of alluvial origins. The predominant climate is semi-cold and semi-humid, with long and cold summers and monsoon rains accompanied by winter precipitation with an annual mean value of 779 mm and mean annual temperatures of 5 to 12 °C.

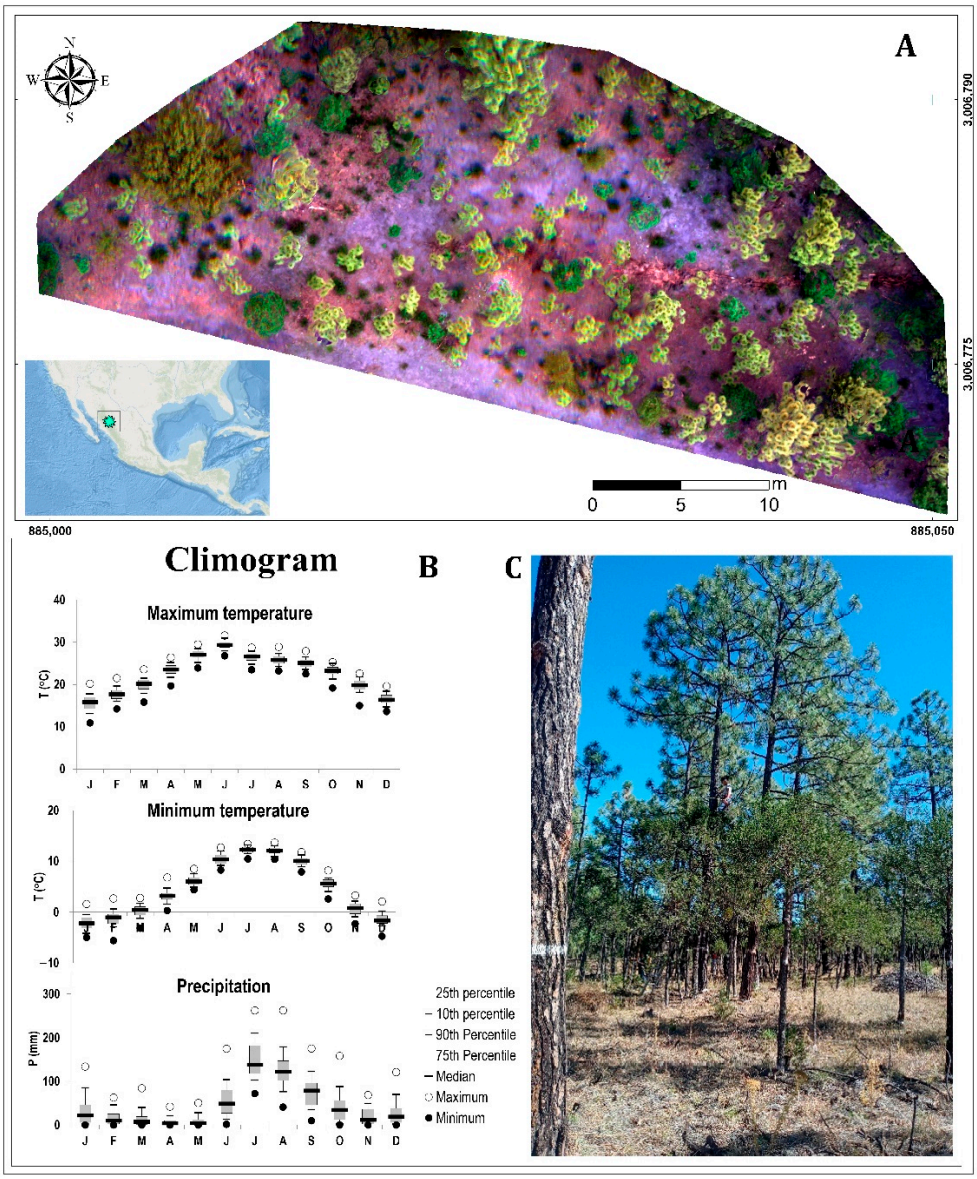

Figure 1. Location and view of Mesa del Pawiranachi (**A**) and climogram of the Papajichi ejido in Chihuahua, Mexico (**B**) and the perspective of site (**C**).

Workflow

To obtain field data during the month of October; each individual tree within the study area was labeled by fixing an aluminum plate to the base. A complete census of all individuals was conducted, recording the following dasometric variables at individual tree level: diameter at breast height (DBH, cm) and basal diameter (BD, cm), using a diametric tape; and commercial height (CH, m) and total height (TH, m), which were measured directly by climbing the trees and using a length meter (Figure 2).

The study area was overflown using a DJI Phantom multispectral (P4M) quadcopter (Figure 2). The P4M camera has a total of six imaging sensors, five of which are multispectral (bands: blue = 450 ± 16 nm, green = 560 ± 16 nm, red = 650 ± 16 nm, RedEdge = 730 ± 16 nm, near-infrared = 840 ± 26 nm) and one RGB sensor, all with a global 2 MP shutter. The UAV was flown in order to obtain and subsequently process 400 aerial photographs of the study area, taken from an altitude of 50 m, with overlaps between the images and lines of 80 and 75%, respectively. A subsequent flight was conducted from east to west in order to capture RGB and spectral images. Both flights were conducted on 16 October 2021, which was a sunny day, with suitable wind conditions (<25 kph) and a mean temperature of 19 °C.

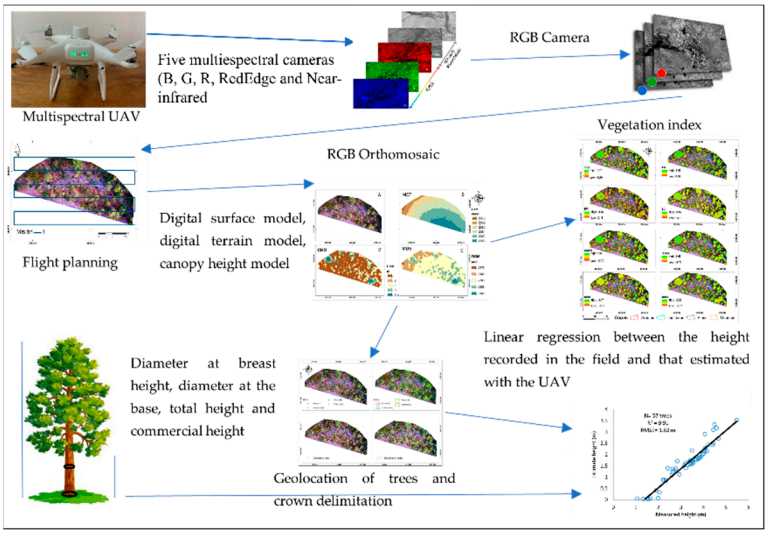

Figure 2. Workflow of the processing stages of images taken by an unmanned aerial vehicle (DJI Phantom 4 Multispectral UAV).

The UAV used had a georeferencing system on board during the flight and it was not necessary to use the real-time-kinematic (RTK) system since the georeferencing system could attain vertical and horizontal location pressures of ±0.1 and ±0.3 m, respectively [22]. For processing, we used a computer with an AMD Ryzen 3900x processor with 24 cores at 3.8 GHz, with an integrated Nvidia Quadro p620 quad-core 2 GHz video card and 32 GB of RAM; this was used in a Linux operating system environment based on the ubuntu distribution Pop!_OS version 22.04 LTS.

The images were processed and analyzed with photogrammetric procedures using the open-source software OpenDroneMap (ODM version: 2.8.4; Cleveland Metroparks, Ohio, USA [23]). This software implements the algorithms Structure from Motion and Multi-View Stereo (SfM and MVS), producing 3D point clouds of 1000–20,000 points m^{-2}. We used VisualSfM to achieve the 3D reconstruction [12], due to its versatility in terms of reduced processing time. We then generated the RGB orthomosaic and multispectral orthomosaic. The digital surface (DSM) was generated considering the maximum elevation values from the trees in a point cloud. Where two points occurred on top of each other, only the tallest point was used. Gaps in the point cloud were filled using the dem-gap fill-steps process with the local gridding method. The digital terrain model (DTM) was obtained by classifying the point cloud using a simple morphological filter (SMRF).

Using the raster calculator tool of the open-source software QGIS, the canopy height model (CHM; Equation (1)) was generated in order to predict the potential height of each tree:

$$CHM = DSM - DTM \quad (1)$$

where CHM = canopy height model, DSM = digital surface model and DTM = digital terrain model.

Analysis of the canopy consisted of detecting and geolocating trees in the study area, estimating their heights and delimiting their crowns to obtain the values of crown diameter and area. The package ForestTools [24] of the statistical software R [25] was used as a tool to geolocate the individual trees and delimit their crowns through the variable window filter (VWF) algorithm and the algorithm of segmentation controlled by markers. This package automatically detects the crowns of the trees, obtains the tree height (TH, m), generates polygons and calculates the area of the crown (Ac, m^2).

Using the multispectral orthophoto, the reflectance level was calculated according to the wavelength of each band. In the QGIS software, the Semi-Automatic Classification

Plugin was executed; this tool allows us to calculate the reflectance of a chosen area according to the values of each band.

Given there are studies that have exhaustively verified their adequacy, and some may be redundant [26,27], we consider it appropriate to analyze them individually in order to obtain a more profound interpretation. Moreover, it has been documented that each is affected by sensor type and atmospheric effects, for which reason multi-analysis provides a rigor that guarantees their replicability and cooperation [28]. The calculation was performed using the raster calculator of the program QGIS through the following expressions (Equations (2)–(9)).

$$\text{NDVI} = \frac{\text{NIR} - \text{RED}}{\text{NIR} + \text{RED}} \tag{2}$$

$$\text{LCI} = \frac{\text{NIR} - \text{RedEdge}}{\text{NIR} + \text{RED}} \tag{3}$$

$$\text{RVI} = \frac{\text{NIR}}{\text{RED}} \tag{4}$$

$$\text{GNDVI} = \frac{\text{NIR} - \text{GREEN}}{\text{NIR} + \text{GREEN}} \tag{5}$$

$$\text{NDRE} = \frac{\text{NIR} - \text{RedEdge}}{\text{NIR} + \text{RedEdge}} \tag{6}$$

$$\text{NDGI} = \frac{\text{GREEN} - \text{RED}}{\text{GREEN} + \text{RED}} \tag{7}$$

$$\text{TVI} = \sqrt{\frac{\text{NIR} - \text{RED}}{\text{NIR} + \text{RED}} + 0.05} \tag{8}$$

$$\text{OSAVI} = \frac{\text{NIR} - \text{RED}}{\text{NIR} + \text{RED} + 0.16} \tag{9}$$

where NDVI = normalized difference vegetation index, GNDVI = green NDVI, LCI = leaf chlorophyll index, NDRE = normalized difference red edge index, OSAVI = optimized soil adjusted vegetation index, RVI = ratio vegetation index, TVI = transformed vegetation index, NDGI = normalized difference greenness index, NIR = near infrared band, RED = red band, RedEdge = red edge band and GREEN = green band.

To evaluate photosynthetic activity within the community, the index values were extracted for the crown of each tree. In order to obtain the statistics per genus, the zone statistics tool of the QGIS program was implemented.

With the exception of the crown, which is a novel parameter not geometrically comparable in the field, estimates of the variables at the individual tree level obtained with the UAV were evaluated with respect to the field measurements. In the case of height, given the operational difficulty of its measurement, a subsample of n = 57 trees was used to evaluate the accuracy of the estimates (https://youtu.be/EIkZQX8qI98; accessed on 22 March 2022). As a validation strategy, we manually digitized 47 trees and compared these with those values derived from the algorithm (Ac).

3. Results

A total of 400 images were obtained with the RGB sensor on a single flight and used to generate the RGB orthomosaic (the processing was 4 min), the digital terrain, the surface models and the canopy height models derived from the photogrammetric process (the processing was 8 min) with the software OpenDroneMap (Figure 3).

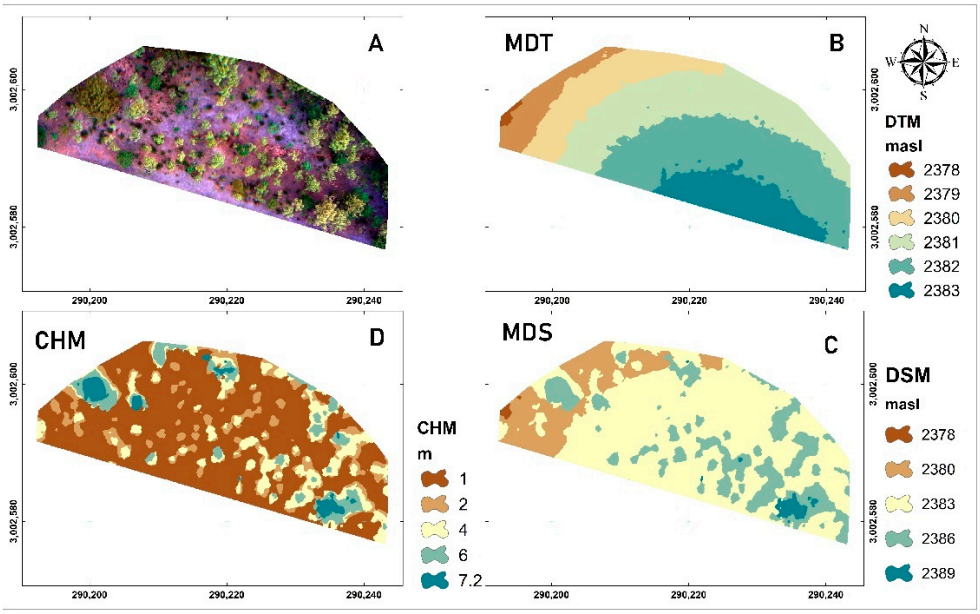

Figure 3. (**A**) = orthomosaic RGB, (**B**) = digital terrain model, (**C**) = digital surface model and (**D**) = canopy height model, derived from the UAV flight.

In the field study, 163 trees in "El Cordoncito" in the Mesa del Pawiranachi were recorded and measured. Table 1 presents the descriptive statistics of the metrics of the individuals taken in the field and calculated in the office. This area is a natural forest and subjected to timber forest management, the individual trees of which present a normal diameter of 1.8 to 62.3 cm with an average of 9.25 cm, and heights of 0.63 to 20.76 m with an average of 4.91 m. This indicates that the population present in "El Cordoncito" is in a state of growth since most of the individuals are juveniles with only a limited number of dominant trees present.

Table 1. Statistical description of the trees recorded in "El Cordoncito".

Variable	CH	TH	Hc	BD	ND
n	163	163	163	163	163
min	1.13	1.91	0.56	4	1.8
q1	1.86	3.495	1.555	9.25	6.2
average	2.211	4.911	2.7	13.064	9.247
median	2.16	4.45	2.18	11.5	8.1
q3	2.41	5.5	3.185	15.05	10.75
max	5.39	15.09	10.41	46.3	37.5
sd	0.664	2.262	1.782	6.446	5.231
se	0.052	0.177	0.14	0.505	0.41

where CH = commercial height (m), TH = total height (m), Hc = height of crown (m), BD = basal diameter (cm), ND = normal diameter (cm), n = number of trees, q1 = quartile 1, q3 = quartile 3, max = maximum, min = minimum, sd = standard deviation and se = standard error.

Statistics were also obtained at the genus level (Table 2). The greatest densities per genus were Pinus, Juniperus, Quercus and Arbutus (109, 43, 9 and 2, respectively), for which reason the forest in the community is Pinus-Juniperus.

Using the variable window filter algorithm of the package ForestTools, 132 trees were detected and their crowns delimited (Figure 4). The algorithm had a tree identification accuracy of 64.4% (163 digitalized–132 detected) with respect to the trees verified in the field. This can be attributed to the heterogeneity of the canopy structures, where some trees underlie the dominant individuals, as well as to the irregular spacing among the trees themselves.

Figure 5 shows the results of the linear regression applied to determine the relationship between the height and crown values recorded in the field and those estimated with the UAV. Furthermore, a graph of dispersion of the residuals of the field data against the predicted values is presented. Statistical evaluations of the characteristics recorded with the field data and those estimated with the UAV showed that 90% of the height and 91% of the crown delineation values are explained by the UAV.

Table 2. Statistical description of the trees recorded in "El Cordoncito".

Genus	Variable	n	min	q1	Average	Median	q3	max	sd	se
Arbutus	CH	2	1.54	1.585	1.63	1.63	1.675	1.72	0.127	0.09
	TH		4.05	4.318	4.585	4.585	4.852	5.12	0.757	0.535
	Hc		2.51	2.732	2.955	2.955	3.178	3.4	0.629	0.445
	BD		12.5	14.125	15.75	15.75	17.375	19	4.596	3.25
	ND		8	9.45	10.9	10.9	12.35	13.8	4.101	2.9
Juniperus	CH	43	1.13	1.43	1.745	1.71	2.03	2.41	0.365	0.056
	TH		1.91	2.58	3.549	3.45	4.47	6.34	1.122	0.171
	Hc		0.56	1.005	1.804	1.57	2.32	4.89	0.876	0.134
	BD		4	6.55	10.667	8.3	14.15	28.8	5.213	0.795
	ND		1.8	3.95	7.174	6.1	10.05	22.6	4.042	0.616
Pinus	CH	109	1.52	2.02	2.429	2.28	2.53	5.39	0.678	0.065
	TH		2.21	3.88	5.33	4.7	6.1	15.09	2.373	0.227
	Hc		0.6	1.75	2.901	2.47	3.32	10.41	1.856	0.178
	BD		6.3	10	13.504	11.6	14.7	46.3	6.025	0.577
	ND		3.9	6.9	9.742	8.2	10.3	37.5	5.141	0.492
Quercus	CH	9	1.66	1.72	1.927	1.92	2.02	2.31	0.208	0.069
	TH		3.3	4.91	6.411	5.86	8.81	10.11	2.446	0.815
	Hc		1.64	2.99	4.484	3.95	6.83	8.01	2.29	0.763
	BD		6.3	11.5	18.6	16.4	19.5	44.7	11.669	3.89
	ND		3.5	7.4	12.789	11.4	14.3	31.3	8.264	2.755

where CH = commercial height (m), Hc = height of crown (m), TH = total height (m), BD = basal diameter (cm), ND = normal diameter (cm), n = number of trees, q1 = quartile 1, q3 = quartile 3, max = maximum, min = minimum, sd = standard deviation and se = standard error.

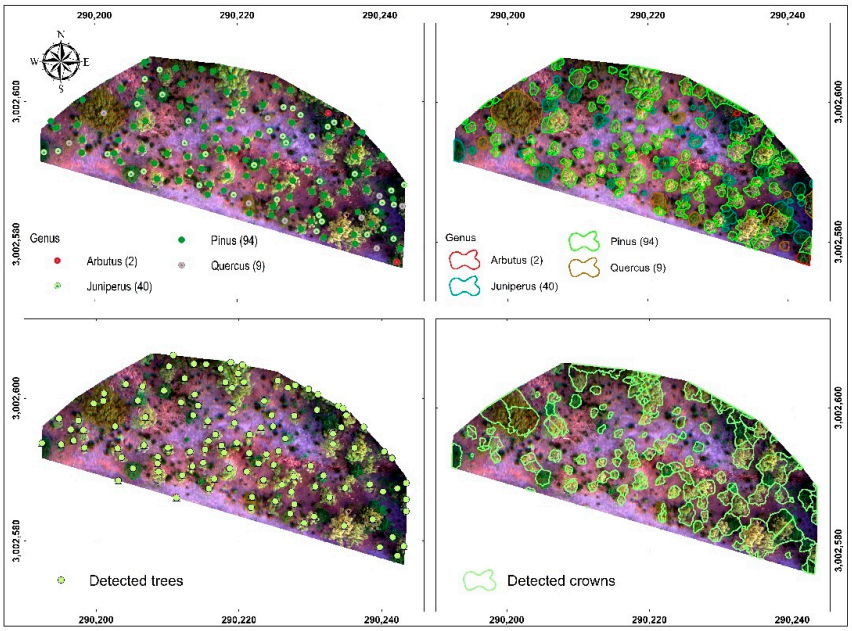

Figure 4. Digitalization of trees (**top left**), digitalization of crowns (**top right**), trees identified (**bottom left**) and crowns detected (**bottom right**) using the ForestTools algorithm.

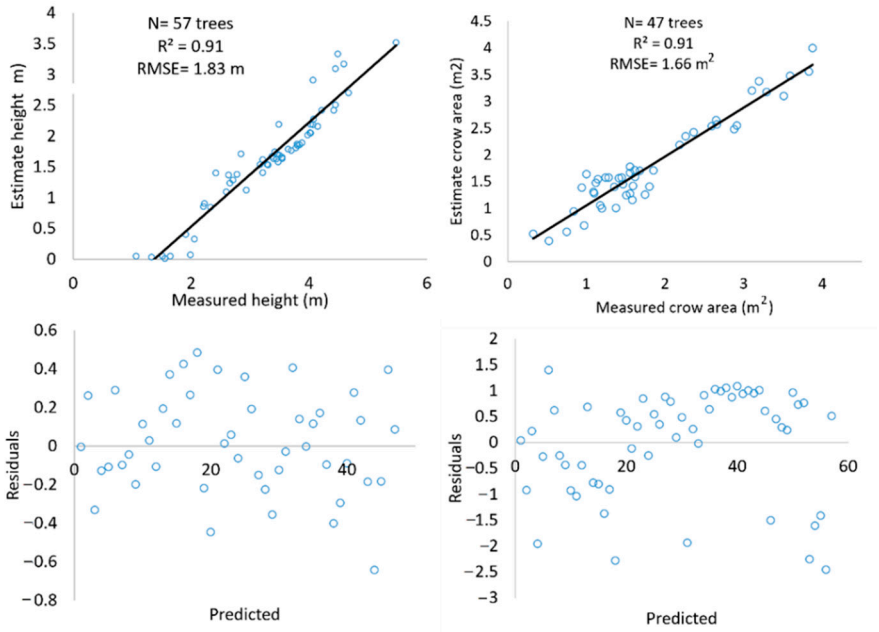

Figure 5. Regression analysis (**top**) and graph of residual vs. predicted values (**bottom**) for height (**left**) and crown delineation (**right**), at individual tree level with field data and estimates derived from the UAV, from 57 trees detected with the ForestTools algorithm.

Three crowns were randomly selected (one of each genus) in order to obtain the multispectral reflectance (Figure 6).

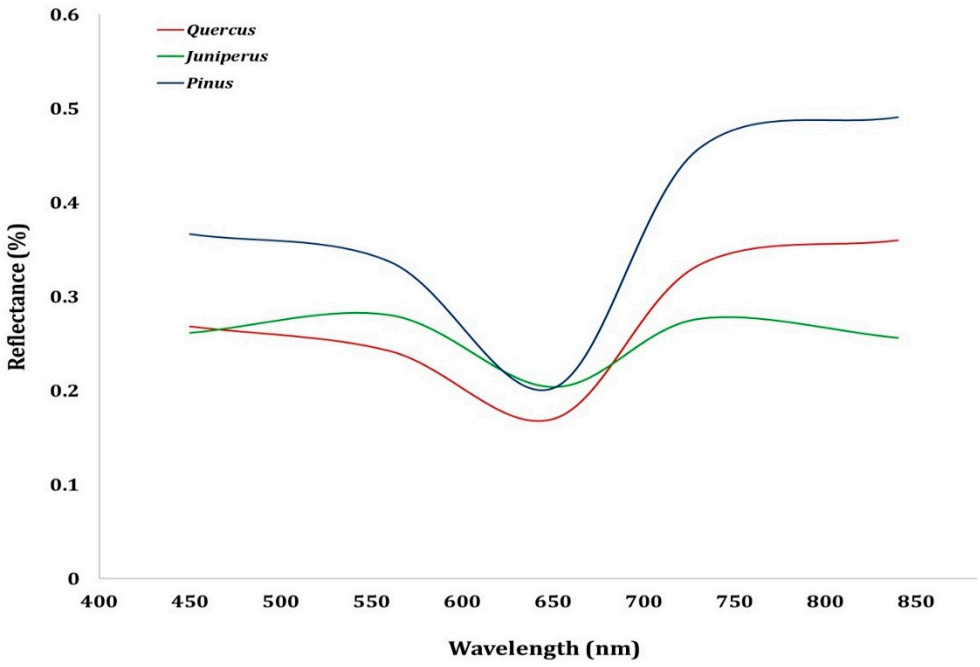

Figure 6. Spectral reflectance at different wavelengths in the crowns of three different genera.

With regard to estimations of the vegetation index, Figure 7 shows the different indices calculated for "El Cordoncito" in Mesa de Pawiranachi from the multispectral orthomosaic derived from the photogrammetric process with OpenDroneMap. Moreover, it was possible to determine the indices NDVI, NDGI, GNDVI, NDRE, OSAVI, LCI, TVI and RVI, obtaining values from −1 to 1, except for RVI, which presented values greater than 1 (Figure 7).

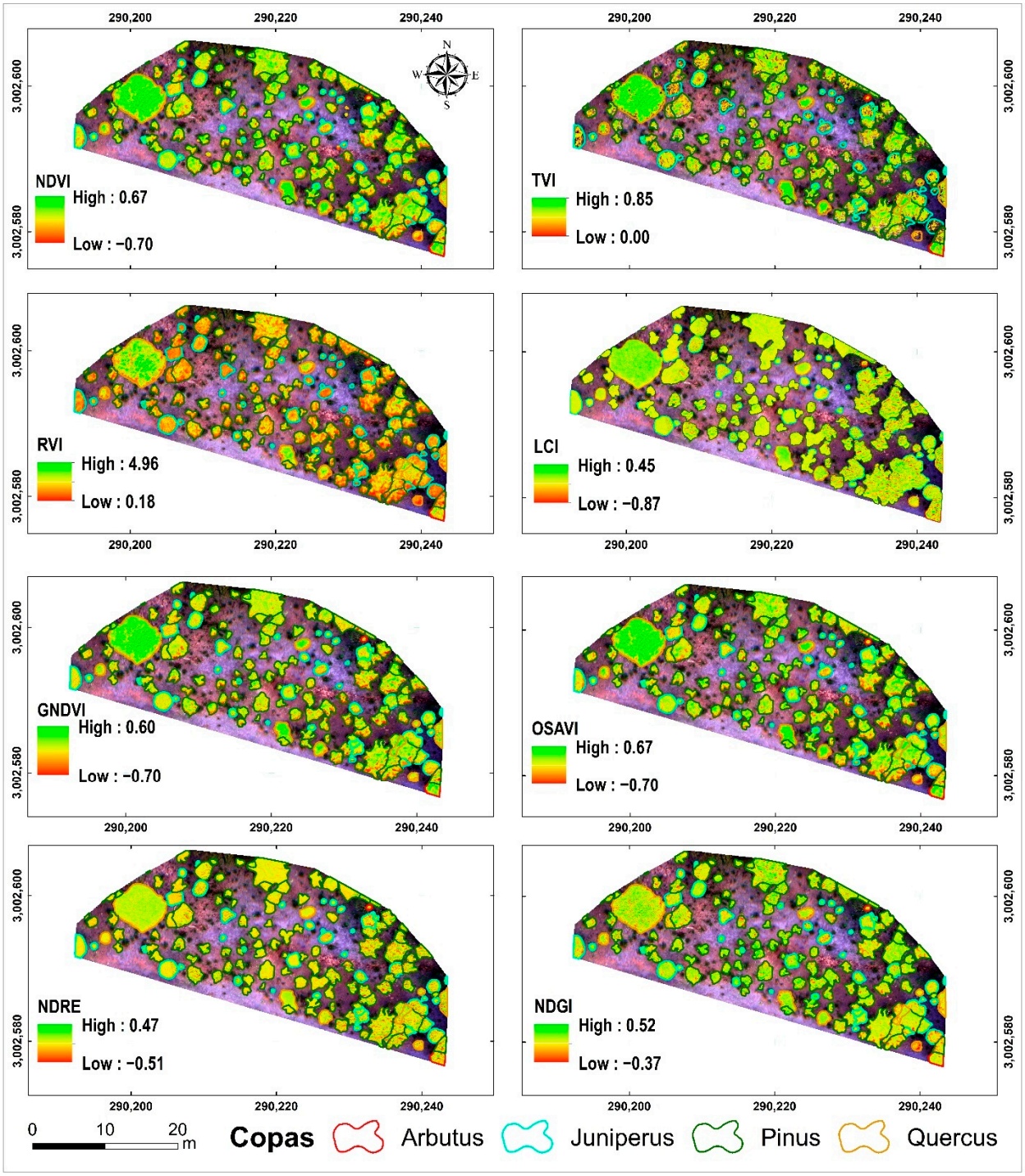

Figure 7. Vegetation indices of "El Cordoncito" in Mesa del Pawiranachi, NDVI = normalized difference vegetation index, GNDVI = green NDVI, LCI = leaf chlorophyll index, NDRE = normalized difference red edge index, OSAVI = optimized soil adjusted vegetation index, RVI = ratio vegetation index, TVI = transformed vegetation index, NDGI = normalized difference greenness index.

For evaluation of the indices according to the delimited trees, NDVI ranged from −0.701 to 0.665, TVI from 0.855 to 0, LCI from 0.48 to −0.95, GNDVI from 0.60 to −0.70, OSAVI from 0.67 to −0.70, NDRE from 0.47 to −0.55, NDGI from 0.47 to −0.55, and RVI from 0 to 4.13 (Figure 7).

The values of the vegetation indices of the crown were visibly higher (green and yellow colors) than the discriminated indices (herbaceous plant vegetation, bare soil, dead vegetal material—orange and red colors). However, both low and high values were found within the tree crowns. These are hypothetically attributable to different levels of photosynthetic activity, as well as open spaces. Figure 8 shows the distribution range of the maximum values of the vegetation indices per genus, which are commonly associated with seasonal extremes in variations of vegetation dynamics [29].

In terms of the distribution of the maximum values of the vegetation indices per genus, Quercus was highest in the indices TVI, NDVI, OSAVI, and LCI (Figures 8 and 9), while Arbutus was highest in NDRE and LCI, and Pinus in NDGI. Juniperus was the lowest across all of the indices (Table 3).

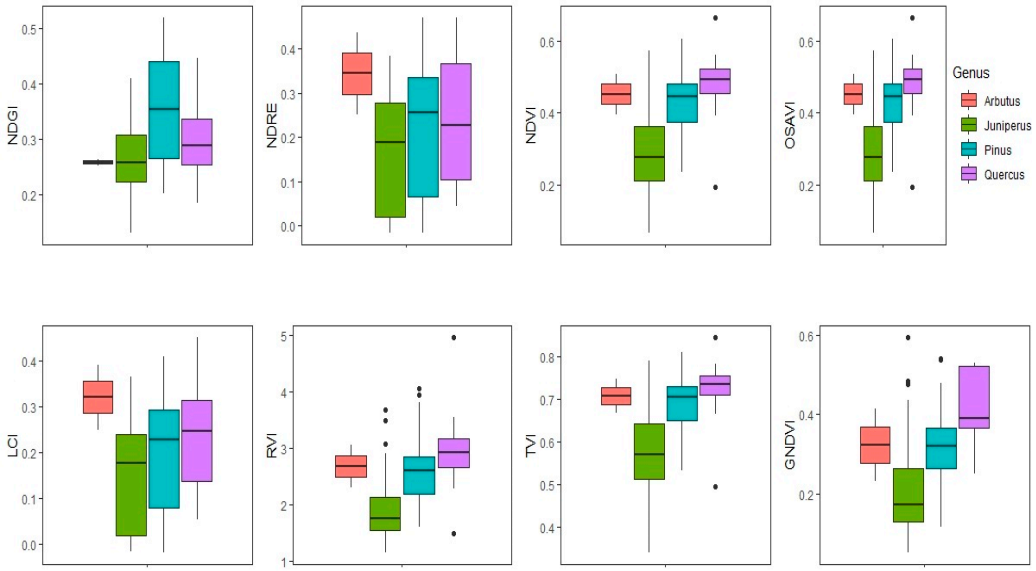

Figure 8. Distribution of the vegetation indices per genus in "El Cordoncito" in Mesa del Pawiranachi, NDVI = normalized difference vegetation index, GNDVI = green NDVI, LCI = leaf chlorophyll index, NDRE = normalized difference red edge index, OSAVI = optimized soil adjusted vegetation index, RVI = ratio vegetation index, TVI = transformed vegetation index, NDGI = normalized difference greenness index.

Table 3. Statistical description of the maximum values of the vegetation indices of the detected crowns.

Variable	GNDVI	LCI	NDGI	NDRE	NDVI	OSAVI	RVI	TVI
min	−0.024	0	−0.347	0	−0.206	−0.206	0.658	0.455
average	0.307	0.198	0.089	0.212	0.412	0.412	2.508	0.680
max	0.596	0.453	0.520	0.472	0.664	0.664	4.96	0. 845
sd	0.109	0.118	0.117	0.141	0.112	0.112	0.598	0.073

where min = minimum, max = maximum, sd = standard deviation, NDVI = normalized difference vegetation index, GNDVI = green NDVI, LCI = leaf chlorophyll index, NDRE = normalized difference red edge index, OSAVI = optimized soil adjusted vegetation index, RVI = ratio vegetation index, TVI = transformed vegetation index, NDGI = normalized difference greenness index.

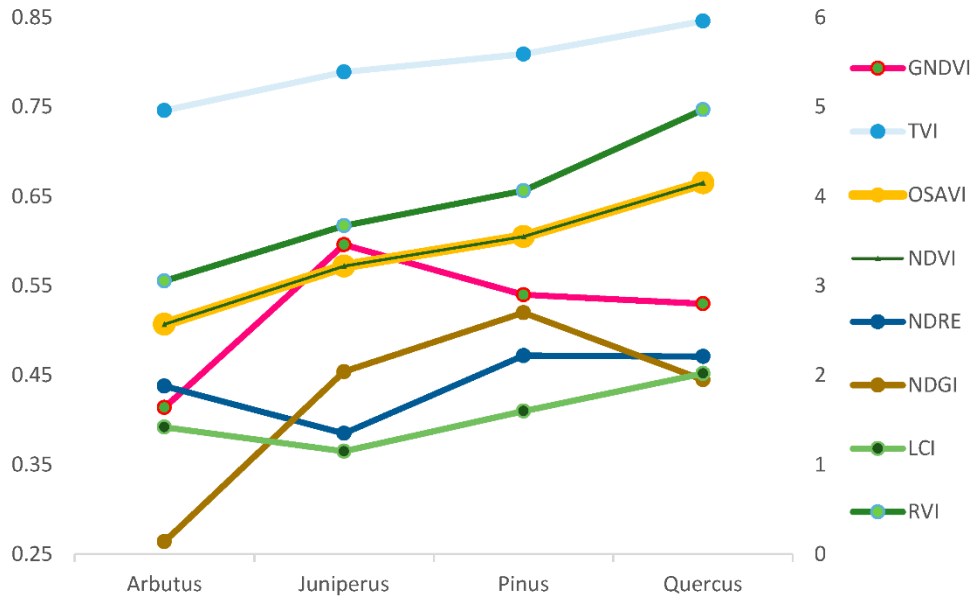

Figure 9. Comparison of the vegetation indices per genus in Mesa del Pawiranachi, NDVI = normalized difference vegetation index, GNDVI = green NDVI, LCI = leaf chlorophyll index, NDRE = normalized difference red edge index, OSAVI = optimized soil adjusted vegetation index, RVI = ratio vegetation index, TVI = transformed vegetation index, NDGI = normalized difference greenness index.

4. Discussion

Modern silviculture aims to optimize resources in the search for sustainable forest management [30]. This study developed procedures for the estimation of attributes at the level of the individual trees that are pioneers in Mexican natural forests. The number of trees, crown area and total height are the main measurements in the forest inventory and are critical to the support of appropriate decision-making. Similarly, multispectral indices were calculated as a strategy with which to improve knowledge of reflectance as an indicator of the ecological mechanisms faced by these ecosystems [31].

The quantification of such structural variables/traits has implications for the fauna in the habitat [32] and, in general, for the ecology of the forest stand [33]. For example, the geometry of the crown and the tree height is directly related to the capacities for carbon capture, while the photosynthetic rates of the trees can provide indications regarding vigor and climatic vulnerability [34]. These aerial parts of the tree represent variables of great ecological interest that merit further investigation in order to contribute to our knowledge.

4.1. Estimation of Attributes of Individual Trees

Regarding estimation of tree-level attributes using UAV technology, our study provides a perspective of such estimation in natural stands. From a practical point of view, this strategy enhances the use of individual tree-level attribute measurements, saves time and improves certainty. In spite of certain shortcomings (addressed below), we demonstrate that, when traditional measurement procedures are combined with UAV-derived geospatial information, knowledge of forest stands is enhanced and decision-making in forest management could be improved as a result. To scale up the potential for application to larger areas of forest, ideal experimentation sites must be identified. We consider that the study area was strategic in terms of the potential extrapolation of the application of the technique to other management scales. For example, the coexistence of four genera within a relatively limited area, together with the dendroecological structural variations present (see Table 2), confers advantages over traditional monospecific and contemporary studies and those of regular spatial arrangement [35].

In the first instance, quantification of the number of trees produced limited results, unlike those found in neighboring areas [12]. This could be explained by the difference in the structural complexity of the stand, as well as in the number of UAV flights performed. However, our findings can provide forest managers with a spatial perspective regarding the density of the forest that could be of utility for the purposes of exploration and planning, and that was previously unavailable or very difficult to achieve at ground level.

Delimitation of the tree crowns using UAV technology constitutes an important metric in biometry with implications for tree physiological development. In the field, the technician normally tries to indirectly estimate this parameter by assuming the area of a circle from the average of the greatest and smallest diameters of the crown. However, the bias inherent in this technique reduces the reliability of the results. For this reason, the estimates generated by the UAV present greater certainty since the algorithm acts to more closely delimit the irregular shape, as seen in [36]. The Structure from Motion (SfM) algorithm has been successfully used in conifer forests; however, its application in mixed forests with broadleaf species is still incipient [37]. Our results are favorable since tree density and distribution can be mapped along with the crown area. These metrics therefore offer an opportunity to influence estimates of biomass and/or carbon [38].

From an ecological perspective, the crown is a multipurpose ecological indicator, including estimates of the potential for carbon capture, aerial biomass storage, forest fire risk, requirements for cultivation work (pruning, thinning, etc.), density regimes, vegetation changes, regeneration strategies, classification of species and refuges for fauna [39,40]. Accurate estimation of the crown dimensions is therefore essential for precision silviculture [41].

One limitation of the detection algorithm is that the segmentation routine is strongly affected by stand characteristics such as density, species heterogeneity, and tree age [37]. Our strategy consisted of smoothing the canopy height model using filters, as seen in [39]. The result allowed better crown delimitation despite the differences in leaf and branch shapes among the studied genera. However, it is important to monitor the intensity of the filters and verify the field data, since small trees may be omitted, as well as those that were being suppressed by the adult trees. It is therefore advisable to complement the analysis with hyperspectral and LiDAR tools [42–44], although the financial implications should also be taken into account. In addition, segmentation techniques need to be refined to delimit the crowns from the tree tops. We therefore recommend conducting thorough initial tree top detection for use as an input to the canopy delimitation process

Although our study did not include an exhaustive analysis of the accuracy of auto-delimitation of the tree crown, we found the estimations to be good (R^2 = 0.91; RMSE = 1.83 m^2). Better results were clearly evident in the broadleaf species, supporting [37]. We attributed this to the fact that this particular leaf foliage gives rise to a homogeneous crown conformation, while the needle and branch arrangement in the conifers gives rise to greater inconsistencies in the segmentation process [44,45]. It is also advisable to differentially evaluate the algorithms according to species, given the variation that exists in the configuration of the irregular geometry that confers differing complexity according to genus.

Accurate height estimation is of crucial importance for both ecological and commercial reasons. It is a significant indicator of the productive capacity of the site and a fundamental requirement for subsequent estimates of stand structure [37]. Our methodology produced acceptable results (R^2 = 0.91, RMSE = 0.36) since, compared to previous studies such as those of [30,45], the statistical values are consistent. Any bias can be attributed to the difficulty in mapping the vegetation and leaf litter below the tree at the time of generating the digital surface model, and subsequent corrections are therefore advisable when field data on leaf litter thickness are available. However, the estimation capabilities of the UAV are significantly better than those of technician-led efforts, since the occlusion and overlapping of canopies make it difficult to accurately distinguish the canopy apex. Another limitation may be the seasonality of the estimations, since some species of the genera Arbutus and Quercus are devoid of foliage at certain times of the year, making it difficult to distinguish

the uppermost tip of the tree. In normative terms, the error found is permissible under current regulations [46].

4.2. Multispectral Indices

Remote sensing is considered one of the most powerful technologies for vegetation assessment. The rapid and vertiginous development of this technology has proven to be an effective tool with which to further our understanding of vegetation dynamics [1,11]. In this study, we extracted the canopy reflectance spectrometry through multispectral indices using UAV at the individual-tree level.

It is recognized that the photosynthetic capacity of canopies is a crucial parameter with which to improve our understanding of the eco-physiological processes taking place between the forest and the atmosphere, i.e., the magnitude of photosynthetic variability in forest species remains a challenge that merits analysis beyond the leaf level, and its accurate estimation would reduce uncertainty in terrestrial biosphere models (e.g., carbon fluxes and others). With no intention of explaining the rates and thresholds of photosynthesis of the studied species, we discuss the spectral reflectance results calculated with multispectral vegetation indices (e.g., VI). This is a preliminary step to further exploring their use and linkage with ground-truth photosynthetic measurements (not measured in this study).

In addition, the spectral reflectance captured by a UAV sensor at canopy level is known to be associated, to a greater extent, with canopy geometry and dispersion of the foliage, etc., often producing spurious spectral variation that can be confused with the spectral signature associated with plant photosynthesis. As discussed below, each index presents differences in its spectral reflectance, but the best combination of these VI remains to be explored. Consequently, we discuss them as a potential source that could predict future photosynthetic productivity [47].

It is noteworthy that, although these VI are not direct measures of actual productivity rates, they are in line with previous studies that use reflectance as a viable tool with which to predict photosynthetic variables, or as an indicator of canopy "greenness" [48], although in this study we only used reflectance spectra and never used leaf-level data or phenological measurements.

In this sense, the NDVI represented the greenness of the individuals and is used by some authors as a proxy for relative biomass [49–51], although it is recommended to determine light use efficiency (LUE). By taking advantage of contrasts between electromagnetic bands and chlorophyll pigments, this index allowed us to differentially distinguish the trees in terms of vigor (Figure 8). The genus Quercus presented the highest values of this index, with advantageous implications for the conservation of this genus in the face of predicted climatic change [52]. Secondly, Pinus and Arbutus seem to share the same level of "greenness", although without very critical conditions. In contrast, the genus Juniperus seems to be the most heavily impacted by environmental or anthropogenic stressors (not studied here). Management strategies such as pruning, thinning, controlled burning and other regimes that could influence site productivity should therefore be considered. The reliability of NDVI in evergreen forests requires further assessment given that previous studies demonstrated uncoupling between NDVI magnitude and productivity due to a change in radiation-use efficiency [48,50,53]

The TVI is sensitive to crown structure [54] and is highly recommended for monitoring changes in the dynamics of the vegetation due to its property of contrasting the values of reflectance [55]. Its values confirmed Quercus as the genus with higher spectral reflectance than the other three genera.

A similar trend was followed by GNDVI, as an indicator of water from soil moisture and nitrogen consumption attributable to photosynthetic activity. Although our study did not contemplate chemical analysis of the soil, previous studies in neighboring sites have reported that nitrogen is not limiting [12]. Consequently, we hypothesized that water will be the limiting factor, as documented by [56,57]. These sites are of shallow soil depth and

water from the monsoon rains tends to run off, leaving the trees under water stress and heavily reliant on winter rains to carry out their physiological processes [58].

The NDRE proved to be a useful complement with which to detect tree anomalies, since it optimizes the detailed data between the red bands and the NIR, complementing the benefits of the NDVI [59]. Thus, Arbutus differed markedly from the other three genera (Figure 8), meaning that this species undergoes marked changes in the properties of its spectral reflectance with respect to the other species. NDRE has been reported as a potential indicator of chlorophyll and changes in photosynthetic rate transitions (not measured here), making it very useful for programming in situ cultural activities that require these plants [59].

The LCI indicated the level of chlorophyll, where the genus Arbutus differed notably from the other genera. According to [13], this index is a good indicator of the leaf area index and is related to the maturity of the individual. For this reason, it merits continuous monitoring.

Regarding the OSAVI, this index evidenced that the highest chlorophyll values are presented by the genus Quercus, followed by Arbutus and the pines, whilst the Juniperus present a small scale. This index considers the soil as a factor of chlorophyll content, such that it is directly related to the amount of canopy foliage [60]. Coincidentally, [61] reports that its values are proportional to the robustness of the canopy. This makes sense since the oaks presented the largest crown dimensions (Table 2). As a consequence, this index could be appropriate for monitoring photosynthetic activity in closed, high-density canopies.

The RVI reflects the fact that the genus Quercus presents the highest chlorophyll values, which is attributed to its greater quantity of foliage and higher crown volume (Figure 8). These results agree with [62], who state that this index is an indicator of chlorophyll content as a factor that influences photosynthesis and nitrogen content.

The NDGI showed the best values for Juniperus and is an indicator [63] of changes in the status quo of the vegetation, e.g., post-disturbance. In other words, this greenness index reflects the reflective characteristics of plants, as determined by their momentary condition. Juniperus differs from other species in terms of cellular structure and moisture and chlorophyll content.

Our spectral multi-indices approach produced greater knowledge of the variation in spectral signatures, as a reflection of the potential photosynthetic activity in the studied trees. As shown in Figure 6, the wavelengths highlight a significant decrease in the percentage of genus-differentiated reflectance around 650 nm. These differences can be interpreted in different ways [63], but it is desirable in the future to take further considerations into account in order to make these data useful for interpretations of photosynthetic activity as such. For example, determination of the radiation use efficiency (RUE) from careful ground measurements would allow a better understanding of the rate of photosynthesis through NDVI. On the other hand, it is necessary to derive continuous spatial and temporal information regarding the tree physiology, complement with hyperspectral data, refine radiometric corrections and calibrate the sensors. This will act to reduce the uncertainty of monitoring the performance of photosynthesis at canopy level, and eventually at leaf level.

We also do not discount the possibility that our results could allow us to discriminate species and phenological processes [64–66]. In any case, it is crucial to determine the behavior of dendroecological variables collected in situ, since multispectral indices are complementary to the field information, which is essential in order to reach better conclusions.

As a limitation, the seasonality of image acquisition should be considered, since there are reports that multispectral indices are also multiseasonal [67]. The dynamics of tree phenology and physiological processes, therefore, merit further study with a temporal perspective. Particularly in the case of oaks, for example, there are seasons when the tree is devoid of foliage while the tree develops other physiological processes, such as root elongation, radial growth, bud development, etc.

Despite the promising results in terms of extracting phenotypic information of high spatial resolution and accurate spectral reflectance for tree-level applications, we highlight certain limiting factors that merit further research. For instance, a range of phenological stages, leaf optical properties, soil reflectance, canopy structure, sun directions, saturation phenomenon, sensor effects, etc. are all important factors governing spectral accuracy [68]. It is therefore advisable to exercise caution with the application of our approach, which is merely descriptive. Before linking multispectral imagery with vigor or tree productivity, fresh consideration of the use of UV-based VI is required. The lack of synchrony between canopy spectrometry and physiological processes means that these indices are not infallible indicators of instantaneous photosynthetic rates. The major problems include atmospheric effects, optical properties and canopy structural attributes, which must be measured in situ. Thus, the combination of VI with environmental and physiological variables requires the adoption of more innovative approaches. In addition, multispectral data acquisition and processing techniques imply high technical requirements and the need for specialized personnel.

5. Conclusions

This research was advantageous for forest monitoring in natural forests and could complement forest inventories and ecology studies. The long time periods required for individual field estimations are drastically reduced by the approach followed here. Our workflow proved to be an effective alternative for characterizing tree attributes. The information generated substantially facilitates applications using the knowledge of the studied species metrics. The accuracy of the metrics is reliable and the multispectral indices are useful indicators of potential photosynthetic capacity. They represent surrogate variables that can be used as input for models of forest ecosystem dynamics. The characterization of VI was a valuable indicator for distinguishing functional genus types. In particular, NDVI is a dominant and effective index for detecting photosynthetic activity, although this does not imply that it is infallible. As a result, one may consider the use of other vegetation indices as generated here.

The quality of the mapping allowed the proposal of new research paradigms, including the need to adjust the algorithms according to tree age, height and species group, since the mapping results were influenced by species composition. Likewise, stand density merits the exploration of additional technologies in order to reduce uncertainty, but the implications in terms of economic costs must be taken into account.

Author Contributions: E.D.V.-V. gathered field data and processing data; M.P.-G. conceived the experiment, lead the data analysis, wrote and edited the original manuscript; J.A.M.-R. processing data; L.A.M.-T. software. All authors have read and agreed to the published version of the manuscript.

Funding: This research was funded by CONACYT for funding provided through project A1-S-21471.

Data Availability Statement: Not applicable.

Acknowledgments: We thank to CONACYT for funding provided through project A1-S-21471, COCYTED and DendroRed, (http://dendrored.ujed.mx; accessed on 15 April 2022). Furthermore, we thank Ejido Papajichi, Andrés Cruz Cruz (El Kapy); Bersaín Acosta Barraza; Martín José Loya Barraza; Manuel de Jesús Espinoza Carrillo; José Pedro Lerma Chacarito; Alexis Arturo Chávez Cervantes; José Flores Hernández y Uriel Bustillos Espino for facilitating and supporting field data gathering.

Conflicts of Interest: The authors declare no conflict of interest.

References

1. Lechner, A.M.; Foody, G.M.; Boyd, D.S. Applications in Remote Sensing to Forest Ecology and Management. *One Earth* **2020**, *2*, 405–412. [CrossRef]
2. Wallerman, J.; Bohlin, J.; Nilsson, M.B.; Franssen, J.E. Drone-Based Forest Variables Mapping of ICOS Tower Surroundings. In *IGARSS 2018–2018 IEEE International Geoscience and Remote Sensing Symposium*; IEEE: Hoboken, NJ, USA, 2018; pp. 9003–9006. [CrossRef]

3. Jayathunga, S.; Owari, T.; Tsuyuki, S. The use of fixed–wing UAV photogrammetry with LiDAR DTM to estimate merchantable volume and carbon stock in living biomass over a mixed conifer–broadleaf forest. *Int. J. Appl. Earth Obs. Geoinf.* **2018**, *73*, 767–777. [CrossRef]
4. Overman, H.; Butt, N.; Cummings, A.R.; Luzar, J.B.; Fragoso, J. National REDD+ Implications for Tenured Indigenous Communities in Guyana, and Communities' Impact on Forest Carbon Stocks. *Forests* **2018**, *9*, 231. [CrossRef]
5. Grybas, H.; Congalton, R.G. A Comparison of Multi-Temporal RGB and Multispectral UAS Imagery for Tree Species Classification in Heterogeneous New Hampshire Forests. *Remote Sens.* **2021**, *13*, 2631. [CrossRef]
6. González, E.; Núñez, C.; Salinas, J.; Rodas, J.; Rodas, M.; Paiva, E.; Kali, Y.; Saad, M.; Lesme, F.; Lesme, J.; et al. Analysis and Application of Multispectral Image Processing Techniques Applied to Soybean Crops from Drones Vision System. In Proceedings of the 18th International Conference on Informatics in Control, Automation and Robotics (ICINCO), Online, 6–8 July 2021; pp. 707–715. [CrossRef]
7. Lausch, A.; Erasmi, S.; King, D.J.; Magdon, P.; Heurich, M. Understanding Forest Health with Remote Sensing-Part I—A Review of Spectral Traits, Processes and Remote-Sensing Characteristics. *Remote Sens.* **2016**, *8*, 1029. [CrossRef]
8. Dash, J.P.; Pearse, G.D.; Watt, M.S. UAV Multispectral Imagery Can Complement Satellite data for Monitoring Forest Health. *Remote Sens.* **2018**, *10*, 1216. [CrossRef]
9. Moncada, W.; Willems, B.; Pereda, A.; Aldana, C.; Gonzales, J. Tendencia anual, anomalías y predicción del comportamiento de cobertura de vegetación con imágenes Landsat y MOD13Q1, microcuenca Apacheta, Región Ayacucho. *Rev. Teledetección* **2022**, *59*, 73–86. [CrossRef]
10. Yu, R.; Luo, Y.; Zhou, Q.; Zhang, X.; Wu, D.; Ren, L. Early detection of pine wilt disease using deep learning algorithms and UAV-based multispectral imagery. *For. Ecol. Manag.* **2021**, *497*, 119493. [CrossRef]
11. Safonova, A.; Hamad, Y.; Dmitriev, E.; Georgiev, G.; Trenkin, V.; Georgieva, M.; Dimitrov, S.; Iliev, M. Individual Tree Crown Delineation for the Species Classification and Assessment of Vital Status of Forest Stands from UAV Images. *Drones* **2021**, *5*, 77. [CrossRef]
12. Gallardo-Salazar, J.L.; Pompa-García, M. Detecting Individual Tree Attributes and Multispectral Indices Using Unmanned Aerial Vehicles: Applications in a Pine Clonal Orchard. *Remote Sens.* **2020**, *12*, 4144. [CrossRef]
13. Liu, S.; Zeng, W.; Wu, L.; Lei, G.; Chen, H.; Gaiser, T.; Srivastava, A.K. Simulating the Leaf Area Index of Rice from Multispectral Images. *Remote Sens.* **2021**, *13*, 3663. [CrossRef]
14. González-Elizondo, M.S.; González-Elizondo, M.; Tena-Flores, J.A.; Ruacho-González, L.; López-Enríquez, I.L. Vegetación de la Sierra Madre Occidental, México: Una síntesis. *Acta Botánica Mex.* **2012**, *100*, 351–403. [CrossRef]
15. Fraser, B.T.; Congalton, R.G. Monitoring Fine-Scale Forest Health Using Unmanned Aerial Systems (UAS) Multispectral Models. *Remote Sens.* **2021**, *13*, 4873. [CrossRef]
16. Jiang, Q.; Fang, S.; Peng, Y.; Gong, Y.; Zhu, R.; Wu, X.; Ma, Y.; Duan, B.; Liu, J. UAV-Based Biomass Estimacion for Rice Combining Spectral, TIN-Based Structural and Meteorological Features. *Remote Sens.* **2019**, *11*, 890. [CrossRef]
17. Marques Ramos, A.P.; Prado Osco, L.; Garcia Furuya, D.E.; Nunes Gonçalves, W.; Cordeiro Santana, D.; Ribeiro Teodoro, L.P.; da Silva Junior, C.A.; Capristo-Silva, G.F.; Li, J.; Rojo Baio, F.H.; et al. A random forest ranking approach to predict yield in maize with uav-based vegetation spectral indices. *Comput. Electron. Agric.* **2020**, *178*, 105791. [CrossRef]
18. Reyes-Zurita, N.; Rodríguez-Ortiz, G.; Enríquez-del Valle, J.R.; Jiménez-Colmenares, C.L.; Rincón-Ramírez, J.A. Estimación de variables dasométricas en rodales bajo manejo forestal con vehículos aéreos no tripulados. *FIGEMPA: Investig. Desarro.* **2022**, *13*, 22–31. [CrossRef]
19. Erb, K.H.; Kastner, T.; Plutzar, C.; Bais, A.L.S.; Carvalhais, N.; Fetzel, T.; Gingrich, S.; Haberl, H.; Lauk, C.; Niedertscheider, M.; et al. Unexpectedly large impact of forest management and grazing on global vegetation biomass. *Nature* **2018**, *553*, 73–76. [CrossRef]
20. Otsu, K.; Pla, M.; Duane, A.; Cardil, A.; Brotons, L. Estimating the Threshold of Detection on Tree Crown Defoliation Using Vegetation Indices from UAS Multispectral Imagery. *Drones* **2019**, *3*, 80. [CrossRef]
21. Fulé, P.Z.; Ramos-Gómez, M.; Cortés-Montaño, C.; Miller, A.M. Fire regime in a Mexican forest under indigenous resource management. *Ecol. Appl.* **2011**, *21*, 764–775. [CrossRef]
22. DJI P4 Multispectral Specs. Available online: https://www.dji.com/p4-multispectral/specs (accessed on 21 March 2022).
23. OpenDroneMap/ODM. Available online: https://github.com/OpenDroneMap/ODM (accessed on 22 February 2022).
24. ForestTools: Analyzing Remotely Sensed Forest Data. Available online: https://CRAN.R-project.org/package=ForestTools (accessed on 22 January 2022).
25. The R Project for Statistical Computing. Available online: https://www.r-project.org/ (accessed on 22 January 2022).
26. Ganivet, E.; Bloomberg, M. Towards rapid assessments of tree species diversity and structure in fragmented tropical forests: A review of perspectives offered by remotely-sensed and field-based data. *For. Ecol. Manag.* **2019**, *432*, 40–53. [CrossRef]
27. Jurado, J.M.; Ortega, L.; Cubillas, J.J.; Feito, F.R. Multispectral Mapping on 3D Models and Multi-Temporal Monitoring for Individual Characterization of Olive Trees. *Remote Sens.* **2020**, *12*, 1106. [CrossRef]
28. Huang, S.; Tang, L.; Hupy, J.P.; Wang, Y.; Shao, G. A commentary review on the use of normalized difference vegetation index (NDVI) in the era of popular remote sensing. *J. For. Res.* **2021**, *32*, 1–6. [CrossRef]
29. Potter, C.S.; Brooks, V. Global analysis of empirical relations between annual climate and seasonality of NDVI. *Int. J. Remote Sens.* **1998**, *19*, 2921–2948. [CrossRef]

30. Hao, Z.; Lin, L.; Post, C.J.; Jiang, Y.; Li, M.; Wei, N.; Yu, K.; Liu, J. Assessing tree height and density of a young forest using a consumer unmanned aerial vehicle (UAV). *New For.* **2021**, *52*, 843–862. [CrossRef]
31. Kureel, N.; Sarup, J.; Matin, S.; Goswami, S.; Kureel, K. Modelling vegetation health and stress using hypersepctral remote sensing data. *Modeling Earth Syst. Environ.* **2022**, *8*, 733–748. [CrossRef]
32. Hardenbol, A.A.; Kuzmin, A.; Korhonen, L.; Korpelainen, P.; Kumpula, T.; Maltamo, M.; Kouki, J. Detection of aspen in conifer-dominated boreal forests with seasonal multispectral drone image point clouds. *Silva Fenn.* **2021**, *55*, 10515. [CrossRef]
33. Jayathunga, S.; Owari, T.; Tsuyuki, S. Digital Aerial Photogrammetry for Uneven-Aged Forest Management: Assessing the Potential to Reconstruct Canopy Structure and Estimate Living Biomass. *Remote Sens.* **2019**, *11*, 338. [CrossRef]
34. Su, J.; Liu, C.; Coombes, M.; Hu, X.; Wang, C.; Xu, X.; Li, Q.; Guo, L.; Chen, W.H. Wheat yellow rust monitoring by learning from multispectral UAV aerial imagery. *Comput. Electron. Agric.* **2018**, *155*, 157–166. [CrossRef]
35. Liu, K.; Shen, X.; Cao, L.; Wang, G.; Cao, F. Estimating forest structural attributes using UAV-LiDAR data in Ginkgo plantations. *ISPRS J. Photogramm. Remote Sens.* **2018**, *146*, 465–482. [CrossRef]
36. Weinstein, B.G.; Marconi, S.; Bohlman, S.A.; Zare, A.; White, E.P. Cross-site learning in deep learning RGB tree crown detection. *Ecol. Inform.* **2020**, *56*, 101061. [CrossRef]
37. Miraki, M.; Sohrabi, H.; Fatehi, P.; Kneubuehler, M. Individual tree crown delineation from high-resolution UAV images in broadleaf forest. *Ecol. Inform.* **2021**, *61*, 101207. [CrossRef]
38. Jones, A.R.; Raja Segaran, R.; Clarke, K.D.; Waycott, M.; Goh, W.S.H.; Gillanders, B.M. Estimating Mangrove Tree Biomass and Carbon Content: A cCmparison of Forest Inventory Techniques and Drone Imagery. *Front. Mar. Sci.* **2020**, *6*, 784. [CrossRef]
39. Panagiotidis, D.; Abdollahnejad, A.; Surový, P.; Chiteculo, V. Determining tree height and crown diameter from high-resolution UAV imagery. *Int. J. Remote Sens.* **2017**, *38*, 2392–2410. [CrossRef]
40. Mohan, M.; Silva, C.A.; Klauberg, C.; Jat, P.; Catts, G.; Cardil, A.; Hudak, A.T.; Dia, M. Individual Tree Detection from Unmanned Aerial Vehicle (UAV) Derived Canopy Height Model in an Open Canopy Mixed Conifer Forest. *Forests* **2017**, *8*, 340. [CrossRef]
41. Corona, P.; Chianucci, F.; Quatrini, V.; Civitarese, V.; Clementel, F.; Costa, C.; Floris, A.; Menesatti, P.; Puletti, N.; Sperandio, G.; et al. Precision forestry: Concepts, tools and perspectives in Italia. *For.-J. Silvic. For. Ecol.* **2017**, *14*, 1–21. [CrossRef]
42. Dalponte, M.; Bruzzone, L.; Gianelle, D. Tree species classification in the Southern Alps based on the fusion of very high geometrical resolution multispectral/hyperspectral images and LiDAR data. *Remote Sens. Environ.* **2012**, *123*, 258–270. [CrossRef]
43. Cunliffe, A.M.; Brazier, R.E.; Anderson, K. Ultra-fine grain landscape-scale quantification of dryland vegetation structure with drone-acquired structure-from-motion photogrammetry. *Remote Sens. Environ.* **2016**, *183*, 129–143. [CrossRef]
44. Zhen, Z.; Quackenbush, L.J.; Zhang, L. Trends in Automatic Individual Tree Crown Detection and Delineation—Evolution of LiDAR Data. *Remote Sens.* **2016**, *8*, 333. [CrossRef]
45. Shashkov, M.; Ivanova, N.; Shanin, V.; Grabarnik, P. Ground Surveys Versus UAV Photography: The Comparison of Two Tree Crown Mapping Techniques. In *Information Technologies in the Research of Biodiversity*; Springer: Cham, Switzerland, 2019; pp. 48–56. [CrossRef]
46. Norma Oficial Mexicana NOM-152-SEMARNAT-2006. Available online: http://www.diariooficial.gob.mx/nota_detalle.php?codigo=5064731&date=17/10/2008 (accessed on 20 March 2022).
47. Meneses, V.A.B.; Téllez, J.M.; Velasquez, D.F.A. Uso de drones para el análisis de imágenes multiespectrales en agricultura de precisión. *Limentech Cienc. y Tecnol. Aliment.* **2015**, *13*, 28–40. [CrossRef]
48. Gamon, J.A.; Field, C.B.; Goulden, M.L.; Griffin, K.L.; Hartley, A.E.; Joel, G.; Penuelas, J.; Valentini, R. Relationships between NDVI, Canopy Structure, and Photosynthesis in Three Californian Vegetation Types. *Ecol. Appl.* **1995**, *5*, 28–41. [CrossRef]
49. Riihimäki, H.; Heiskanen, J.; Luoto, M. The effect of topography on arctic-alpine aboveground biomass and NDVI patterns. *Int. J. Appl. Earth Obs. Geoinf.* **2017**, *56*, 44–53. [CrossRef]
50. Liu, S.; Cheng, F.; Dong, S.; Zhao, H.; Hou, X.; Wu, X. Spatiotemporal dynamics of grassland aboveground biomass on the Qinghai-Tibet Plateau based on validated MODIS NDVI. *Sci. Rep.* **2017**, *7*, 4182. [CrossRef]
51. Han, H.; Wan, R.; Li, B. Estimating Forest Aboveground Biomass Using Gaofen-1 Images, Sentinel-1 Images, and Machine Learning Algorithms: A Case Study of the Dabie Mountain Region, China. *Remote Sens.* **2022**, *14*, 176. [CrossRef]
52. Alla, A.Q.; Pasho, E.; Marku, V. Growth variability and contrasting climatic responses of two Quercus macrolepis stands from Southern Albania. *Trees* **2017**, *31*, 1491–1504. [CrossRef]
53. Vicente-Serrano, S.M.; Camarero, J.J.; Olano, J.M.; Martín-Hernández, N.; Peña-Gallardo, M.; Tomás-Burguera, M.; Gazol, A.; Azorin-Molina, C.; Bhuyan, U.; Kenawy, A.E. Diverse relationships between forest growth and the Normalized Difference Vegetation Index at a global scale. *Remote Sens. Environ.* **2016**, *187*, 14–29. [CrossRef]
54. Cui, B.; Zhao, Q.; Huang, W.; Song, X.; Ye, H.; Zhou, X. A New Integrated Vegetation Index for the Estimation of Winter Wheat Leaf Chlorophyll Content. *Remote Sens.* **2019**, *11*, 974. [CrossRef]
55. Σκιάνης, Γ.Α.; Βαιόπουλος, Δ.Α.; Νικολακόπουλος, Κ. Assessment of the TVI vegetation index with the aid of probability theory. *Geol. Soc. Am. Bull.* **2004**, *36*, 1338–1346. [CrossRef]
56. Girolimetto, D.; Venturini, V. Water Stress Estimation from NDVI-Ts Plot and the Wet Environment Evapotranspiration. *Adv. Remote Sens.* **2013**, *2*, 283–291. [CrossRef]
57. Thapa, S.; Rudd, J.C.; Xue, Q.; Bhandari, M.; Reddy, S.K.; Jessup, K.E.; Liu, S.; Devkota, R.N.; Baker, J.; Baker, S. Use of NDVI for characterizing winter wheat response to water stress in a semi-arid environment. *J. Crop Improv.* **2019**, *33*, 633–648. [CrossRef]

58. Pompa-García, M.; Camarero-Martínez, J.J. Potencial dendroclimático de la madera temprana y tardía de *Pinus cooperi* Blanco. *Agrociencia* **2015**, *49*, 177–187. Available online: http://www.scielo.org.mx/pdf/agro/v49n2/v49n2a6.pdf (accessed on 12 February 2022).
59. Jorge, J.; Vallbé, M.; Soler, J.A. Detection of irrigation inhomogeneities in an olive grove using the NDRE vegetation index obtained from UAV images. *Eur. J. Remote Sens.* **2019**, *52*, 169–177. [CrossRef]
60. Lei, S.; Luo, J.; Tao, X.; Qiu, Z. Remote Sensing Detecting of Yellow Leaf Disease of Arecanut Based on UAV Multisource Sensors. *Remote Sens.* **2021**, *13*, 4562. [CrossRef]
61. Steven, M.D. The Sensitivity of the OSAVI Vegetation Index to Observational Parameters. *Remote Sens. Environ.* **1998**, *63*, 49–60. [CrossRef]
62. Qi, H.; Wu, Z.; Zhang, L.; Li, J.; Zhou, J.; Jun, Z.; Zhu, B. Monitoring of peanut leaves chlorophyll content based on drone-based multispectral image feature extraction. *Comput. Electron. Agric.* **2021**, *187*, 106292. [CrossRef]
63. Nedkov, R. Normalized Differential Greenness Index for Vegetation Dynamics Assessment. *Comptes Rendus De L'academie Bulg. Des Sci.* **2017**, *70*, 1143–1146. Available online: https://www.researchgate.net/profile/R-Nedkov-2/publication/319141286_Normalized_differential_greenness_index_for_vegetation_dynamics_assessment/links/5994608d0f7e9b98953af1d6/Normalized-differential-greenness-index-for-vegetation-dynamics-assessment.pdf (accessed on 22 February 2022).
64. De Castro, A.I.; Torres-Sánchez, J.; Peña, J.M.; Jiménez-Brenes, F.M.; Csillik, O.; López-Granados, F. An Automatic Random Forest-OBIA Algorithm for Early Weed Mapping between and within Crop Rows Using UAV Imagery. *Remote Sens.* **2018**, *10*, 285. [CrossRef]
65. Liu, H. Classification of urban tree species using multi-features derived from four-season RedEdge-MX data. *Comput. Electron. Agric.* **2022**, *194*, 106794. [CrossRef]
66. Li, L.; Mu, X.; Chianucci, F.; Qi, J.; Jiang, J.; Zhou, J.; Chen, L.; Huang, H.; Yan, G.; Liu, S. Ultrahigh-resolution boreal forest canopy mapping: Combining UAV imagery and photogrammetric point clouds in a deep-learning-based approach. *Int. J. Appl. Earth Obs. Geoinf.* **2022**, *107*, 102686. [CrossRef]
67. Wan, L.; Cen, H.; Zhu, J.; Zhang, J.; Zhu, Y.; Sun, D.; Du, X.; Zhai, L.; Weng, H.; Li, Y.; et al. Grain yield prediction of rice using multi-temporal UAV-based RGB and multispectral images and model transfer—A case study of small farmlands in the South of China. *Agric. For. Meteorol.* **2020**, *291*, 108096. [CrossRef]
68. Asner, G.P. Biophysical and Biochemical Sources of Variability in Canopy Reflectance. *Remote Sens. Environ.* **1998**, *64*, 234–253. [CrossRef]